Hz), 5.19 (dd, 1 H, J = 1.10 and 17.2 Hz), 5.90 (m, 1 H), 7.30 (m, 5 H); ^{13}C NMR ($CDCl_3$) δ 36.3, 58.0, 61.7, 117.7, 125.5, 128.0, 128.4, 132.7, 137.4; MS m/z 160 (M^+); HRMS m/z calcd for $C_{11}H_{12}O$ (M^+) 160.0888, found 160.0890.

Synthesis of Authentic 6a and 6b. To a THF solution (3.0 mL) of a mixture of **8a** and **8b** (65:35) (271 mg, 1.0 mmol) was added BuLi (2.5 N in hexanes, 0.44 mL, 1.1 mmol) at 0 °C. The solution was stirred for 10 min, and tosyl chloride (247 mg, 1.3 mmol) was added at this temperature. The reaction mixture was stirred for 30 min at room temperature. PhSLi was prepared by mixing PhSH (551 mg, 5 mmol) and BuLi (2.5 N in hexanes, 2 mL, 5 mmol) in THF (3 mL). This solution was added to the above reaction mixture, and the resulting solution was stirred for 3 h at room temperature. The reaction mixture was diluted with benzene and washed with water, 1 N NaOH, and brine. The organic layer was dried (Na_2SO_4) and evaporated. Column chromatography of the residue (90:10 hexane–benzene) provided **6** (101 mg, 28%, **6a**/**6b** = 60:40 based on HPLC, column C, 70:30 CH_3CN–H_2O). HPLC separation (column D, 80:20 CH_3CN–H_2O) of the product gave pure **6a** and **6b**. **6a**: ^{1}H NMR ($CDCl_3$) δ 2.05 (m, 1 H), 2.88 (m, 1 H), 3.51 (ddd, 1 H, J = 4.39, 4.76, and 9.16 Hz), 4.41 (d, 1 H, J = 4.76 Hz), 5.06 (m, 2 H), 5.87 (m, 1 H), 7.20–7.40 (m, 15 H); (C_6D_6) δ 2.20 (m, 1 H), 3.00 (m, 1 H), 3.65 (ddd, J = 4.40, 4.76, and 8.79 Hz), 4.61 (d, 1 H, J = 4.76 Hz), 5.05 (m, 2 H), 5.95 (m, 1 H), 6.90–7.40 (m, 15 H); ^{13}C NMR ($CDCl_3$) δ 35.0, 53.4, 56.6, 117.5, 126.8, 127.3, 127.5, 127.9, 128.8, 128.9, 129.1, 131.4, 132.7, 134.6, 135.0, 135.3, 138.2; MS m/z 362 (M^+); HRMS m/z calcd for $C_{23}H_{22}S_2$ (M^+) 362.1163, found 362.1184. Anal. Calcd for $C_{23}H_{22}S_2$: C, 76.20; H, 6.12. Found: C, 76.44; H, 6.02. **6b**: ^{1}H NMR ($CDCl_3$) δ 2.54 (m, 2 H), 3.61 (q like, 1 H, J = 6.23 Hz), 4.40 (d, 1 H, J = 6.23 Hz), 5.15 (m, 2 H), 5.90 (m, 1 H), 7.10–7.40 (m, 15 H); (C_6D_6) δ 2.66 (m, 2 H), 3.72 (q like, 1 H, J = 6.59 Hz), 4.52 (d, 1 H, 6.59 Hz), 5.12 (m, 2 H), 5.91 (m, 1 H), 6.90–7.40 (m, 15 H); ^{13}C NMR ($CDCl_3$) δ 36.8, 55.4, 57.5, 117.9, 126.9, 127.1, 127.4, 128.0, 128.6, 128.8, 131.9, 132.6, 134.9, 135.0, 135.3, 139.5; MS m/z 362 (M^+); HRMS m/z calcd for $C_{17}H_{17}S$ ($M^+ - C_6H_5S$) 253.1051, found 253.0963. Anal. Calcd for $C_{23}H_{22}S_2$: C, 76.20; H, 6.12. Found: C, 76.54; H, 6.10.

Acknowledgment. This work was partially supported by Grant-in-Aid from The Ministry of Education, Science, and Culture, Japan. We also thank M. Inoue, T. Matsui, and M. Kanemoto for their technical assistance.

Registry No. **1a**, 129756-71-4; **1b**, 129732-83-8; **2**, 129732-86-1; **3a**, 762-72-1; **3b**, 762-66-3; **3c**, 762-73-2; **3d**, 24850-33-7; **3e**, 76-63-1; **4**, 27607-77-8; **5a**, 129732-84-9; **5b**, 129732-85-0; **6a**, 129732-87-2; **6b**, 129732-88-3.

Supplementary Material Available: ^{1}H or ^{13}C NMR spectra for **1a,b**, **2**, **7a,b**, **8a,b**, **9a,b**, and (*Z*)- and (*E*)-1-acetoxy-2-methoxy-1-phenylethenes (11 pages). Ordering information is given on any current masthead page.

Conformational Study of Cinchona Alkaloids. A Combined NMR and Molecular Orbital Approach

Gerard D. H. Dijkstra, Richard M. Kellogg,* and Hans Wynberg*

Department of Organic Chemistry, University of Groningen, Nijenborgh 16, 9747 AG Groningen, The Netherlands

Received June 12, 1990

1D and 2D NMR techniques have been used to elucidate the conformational behavior of cinchona alkaloids in solution. Deoxy, chloro, methoxy, and benzoyl derivatives have been studied together with the unsubstituted alkaloids. Semiempirical molecular orbital calculations (AM1) on segments as well as on the complete structures of cinchona alkaloids have given complementary quantitative information. These calculational results have been used to rationalize the experimentally obtained conformational data and to shed light on the subtilities involved that determine the conformation of cinchona alkaloids.

Introduction

Cinchona alkaloids[1] possess a rich chemical tradition. They are isolated from the bark of several species of Cinchona and Remeyia trees, native to the eastern slopes of the Andes. When, in the beginning of the 17th century, Europeans became aware of the action of powdered bark of these trees against fever, the major component, quinine, soon belonged among the most used drugs.[2] A role for cinchona alkaloids in organic chemistry was firmly established with the discovery of their potential as resolving agents.[3] Our interest in these alkaloids started in the 1970s, when we began to appreciate their great potential as chiral catalysts in asymmetric Michael additions.[4] Numerous examples have followed of reactions in which cinchona alkaloids induce asymmetry.[5] We note, however, that an example of an asymmetric synthesis using these alkaloids as catalyst was first reported in 1912.[6]

In all these examples of use of cinchona alkaloids their ability for intimate interaction, discrimination, and recognition are crucial to their success. Detailed knowledge of the conformational behavior of the cinchona alkaloids

(1) For a general review on the chemistry of cinchona alkaloids, see: Grethe, G.; Uskokovic, M. R. In *Heterocyclic Compounds, The Monoterpenoid Indole Alkaloids*; John Wiley and Sons Inc.: New York, 1983; Vol. 25, Part 4, Chapter XII, p 729 and references cited therein.

(2) For other examples of pharmaceutical usage of cinchona alkaloids see: Goodman, L. S.; Gilman, A. G. *The Pharmacological Basis of Therapeutics*, 7th ed.; McMillan Publishing Co.: New York, 1985; pp 756, 1041.

(3) The first resolution ever made was carried out with quinicine and cinchonicine, which are derivatives of quinine and cinchonine. Since then, about 25% of all resolutions have been carried out with cinchona alkaloids. Pasteur, L. *C. R. Acad. Sci.* **1853**, *37*, 110. Wynberg, H. *Top. Stereochem.* **1986**, *16*, 87. Many examples of the use cinchona alkaloids as resolving agents are given by Wilen, S. H. In *Tables of Resolving Agents and Optical Resolutions*; University of Notre Dame Press: London, 1972. Jacques, J.; Collet, A.; Wilen, S. H. In *Enantiomers, Racemates and Resolution*; John Wiley and Sons Inc.: New York, 1981; pp 254, 257.

(4) Helder, R.; Wynberg, H. *Tetrahedron Lett.* **1975**, 4057.

(5) See for example: Wynberg, H. *Top. Stereochem.* **1986**, *16*, 87. Wynberg, H.; Helder, R. *Tetrahedron Lett.* **1975**, 4057. Hummelen, J. C.; Wynberg, H. *J. Org. Chem.* **1979**, *44*, 2238. Marsman, B.; Wynberg, H. *J. Org. Chem.* **1979**, *44*, 2312. Pluim, H.; Wynberg, H. *J. Org. Chem.* **1980**, *45*, 2498. Hiemstra, H.; Wynberg, H. *J. Am. Chem. Soc.* **1981**, *103*, 417. Staring, A. G. J.; Wynberg, H. *J. Am. Chem. Soc.* **1982**, *104*, 166. Staring, A. G. J.; Wynberg, H. *J. Chem. Soc., Chem. Commun.* **1984**, 1181. Hughes, D. L.; Dolling, U. H.; Ryan, K. M.; Schoenewaldt, E. F.; Grabowski, E. J. J. *J. Org. Chem.* **1987**, *52*, 4745. Brzostowska, M.; Gawronski, J. *Monath. fur Chem.* **1984**, *115*, 1373. Soai, K.; Watanabe, M.; Koyano, M. *J. Chem. Soc., Chem. Commun.* **1989**, 534. Trost, B. M.; Shuey, C. D.; Dininno, F., Jr. *J. Am. Chem. Soc.* **1979**, *101*, 1284. Dolling, U. H.; Davis, P.; Grabowski, E. J. J. *J. Am. Chem. Soc.* **1984**, *106*, 446. Jacobsen, E. J.; Marko, I.; Mungall, W. S.; Schroder, G; Sharpless, K. B *J. Am. Chem. Soc.* **1988**, *11*, 1968. Wai, J. S. M.; Marko, I.; Svendsen, J. S.; Finn, M. G.; Jacobsen, E. N.; Sharpless, K. B. *J. Am. Chem. Soc.* **1989**, *111*, 1123.

(6) Bredig, G.; Fiske, P. S. *Biochem. Z.* **1912**, *46*, 7.

0022-3263/90/1955-6121$02.50/0

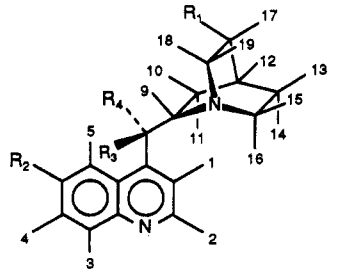

	R_1	R_2	R_3	R_4
quinine	C_2H_3	OCH_3	OH	H
cinchonidine	C_2H_3	H	OH	H
dihydroquinine	C_2H_5	OCH_3	OH	H
dihydrocinchonidine	C_2H_5	H	OH	H
epiquinine	C_2H_3	OCH_3	H	OH
benzoylquinine	C_2H_3	OCH_3	OBz	H
(p-Cl)-benzoyldihydroquinine	C_2H_5	OCH_3	pClBzO	H
chloroquinine	C_2H_3	OCH_3	Cl	H
deoxycinchonidine	C_2H_3	H	H	H

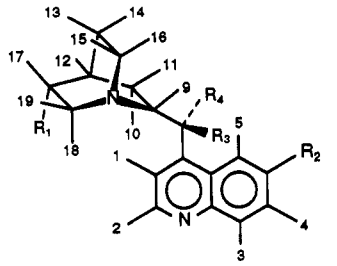

	R_1	R_2	R_3	R_4
quinidine	C_2H_3	OCH_3	OH	H
cinchonine	C_2H_3	H	OH	H
dihydroquinidine	C_2H_5	OCH_3	OH	H
dihydrocinchonine	C_2H_5	H	OH	H
epiquinidine	C_2H_3	OCH_3	H	OH
epidihydroquinidine	C_2H_5	OCH_3	H	OH
(p-Cl)-benzoyldihydroquinidine	C_2H_5	OCH_3	pClBzO	H
acetyldihydroquinidine	C_2H_5	OCH_3	OAc	H
(dimethylcarbamoyl)dihydroquinidine	C_2H_5	OCH_3	OCONMe	H
methoxydihydroquinidine	C_2H_5	OCH_3	OMe	H

Figure 1. Structure, proton numbering, and configuration of the cinchonal alkaloids that have been considered in this study. Note that the skeletal atom numbering (not shown) does not correspond with the proton numbering.

is of utmost importance in explaining these phenomena.

In two papers we have already presented a number of conformational data on cinchona alkaloids in solution, in the gas phase, and in the solid state.[7] In the present work the conformational picture in solution is filled in more completely with new information. This conformational behavior is tested against the results from molecular orbital (MO) calculations on some cinchona derivatives and model compounds. From these calculational results we are now able to understand in some detail the experimental observations. A subtle symphony of solute–alkaloid interactions, together with intramolecular steric interactions, determine the conformation and thus the ability to act as a catalyst, resolving agent, or drug. This symphony can be orchestrated.

Results

Cinchona alkaloids are composed of two relatively rigid entities, an aromatic quinoline ring and an aliphatic quinuclidine ring, connected by two carbon–carbon single bonds.[8] Cinchona alkaloids contain five asymmetric atoms (C_3, C_4, C_8, C_9, and N_1); however, they differ in configuration only at C_8 and C_9.[9] As a result cinchona alkaloids are pairwise related. For example, although morphologically nearly mirror images, quinine and quinidine form a diastereomeric pair. Quinine and quinidine are sometimes called "pseudoenantiomers" for reasons emphasized in Figure 1. In this figure are given the structures, configuration, and proton numbering of the cinchona alkaloids and their derivatives that we have considered in the present study. Most cinchona alkaloids may differ structurally at three positions; a methoxy group is present or absent at C_6' of the quinoline ring (R_2); a vinyl or ethyl group is present at C_3 of the quinuclidine ring (R_1); and different substituents may be introduced at C_9 (R_3, R_4).

Table I.[a] Results of the Conformational Study of Cinchona Alkaloids in Solution[11]

(dihydro)quinine,* (dihydro)quinidine,* (dihydro)cinchonine, and (dihydro)cinchonidine	open conf 3 in all solvents
(dihydro)methoxyquinidine*	both open conf 3 and closed conf 2; in $CDCl_3$ conf 3 in excess, in CD_2Cl_2 conf 2 in excess
benzoylquinine, dihydro-*p*-chlorobenzoylquinine,* dihydro-*p*-chlorobenzoylquinidine,* dihydroacetylquinidine	both open conf 3 and closed conf 2; in all solvents except CD_3OD, conf 2 in excess, but in CD_3OD conf 3 in excess
(dihydro)chloroquinine, (dihydro)chloroquinidine	closed conf 2 with small amounts (<10%) open conf 3 in all solvents
deoxycinchonidine	both open and 3 and closed conf 1 (≈60/40 ratio)
epi(dihydro)quinine,* epi(dihydro)quinidine*	open conf 4

[a] Solvents that have been used: $CDCl_3$, CD_2Cl_2, CD_3COCD_3, C_6D_6, CD_3OD.

NMR Analysis

For the conformational study of cinchona alkaloids in solution the NMR techniques correlation spectroscopy (COSY), nuclear Overhauser enhancement spectroscopy (NOESY), NOE-difference, and vicinal J couplings have been used. The COSY experiments were necessary for the assignments of the ^1H NMR spectra of the cinchona alkaloids. From NOESY and NOE-difference spectra we determined the conformation(s) of the alkaloids. The vicinal J couplings provided additional conformational information. Especially the NOE's between protons of the quinoline ring and the quinuclidine ring proved to be useful for the assignment of the conformations.

From a molecular mechanics study[7] we already know that cinchona alkaloids can in principle adopt four different conformations; two "open" conformations in which the quinuclidine nitrogen points away from the quinoline ring and two "closed" conformations in which the quinuclidine nitrogen points toward the quinoline ring. We will refer frequently to these four different conformations, depicted in Figure 2 for quinidine, during the following discussion.

The main results of the conformational analysis in solution are summarized in Table I. Those data marked with an asterisk have been reported earlier by us;[7] however, they are further refined here and will be used for the interpretative work in the discussion.

(7) Dijkstra, G. D. H.; Kellogg, R. M.; Wynberg, H. *Recl. Trav. Chim. Pays-Bas* **1989**, *108*, 195. Dijkstra, G. D. H.; Kellogg, R. M.; Wynberg, H.; Svendsen, J. S.; Marko, I.; Sharpless, K. B. *J. Am. Chem. Soc.* **1989**, *111*, 8070.

(8) The elucidation of the structure of cinchona alkaloids was reported in 1907: Rabe, P. *Chem. Ber.* **1907**, *40*, 3655.

(9) Prelog concluded that for cinchona alkaloids the C_9 and C_8 carbon atoms have erythro arrangements, whereas for the epicinchona alkaloids a threo relationship exits: Prelog, V.; Hafliger, O. *Helv. Chim. Acta* **1950**, *33*, 2021. Prelog, V. *Tetrahedron Lett.* **1964**, 2037.

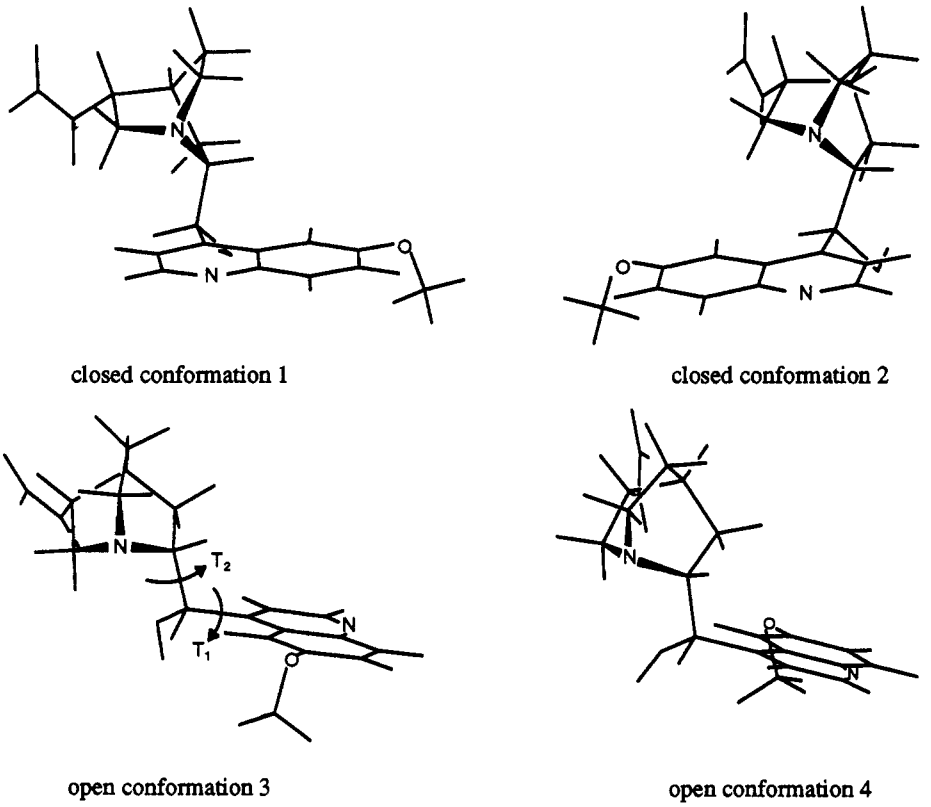

Figure 2. The four minimum energy conformations of quinidine.

Table II. ^{1}H NMR Chemical Shifts (in ppm)[a]

H	A	B	C	D	E	F
1	6.93	7.27	7.55	7.43	7.58–7.20	7.12–6.95
2	8.81	8.80	8.62	8.72	8.77	8.70
3	8.39	8.11	7.96	8.02	8.06	8.26
4	7.37	7.69	7.42	7.38	7.41	7.21
5	7.93	8.05	7.60	7.53	7.58–7.20	7.60–7.40
6	7.24	7.56	–	–	–	–
8a	3.15	3.40	6.79	6.75	5.60–5.30	5.56–5.26
8b	2.69	3.07	–	–	–	–
9	3.03	3.2	3.45	3.49	3.70–3.42	3.60–3.40
10	1.60	1.81	1.84	1.95	1.55	1.27
11	0.83	1.16	1.84	1.73	0.70	0.43
12	1.48	1.75	1.84	1.89	1.66	1.27
13	1.18	1.65	1.58	1.58	1.55	1.08
14	1.29	1.58	1.84	1.80	1.55	1.08
15	2.46	2.78	2.64	2.72	2.9	2.57
16	2.89	3.2	3.23	3.21	3.22	3.02
17	1.94	2.26	2.31	2.30	2.30	1.92
18	2.51	2.67	2.71	2.66	2.9	2.38
19	2.95	3.2	3.04	3.09	3.39	3.10
20	5.58	5.78	5.80	5.84	5.80	5.59
21	4.9	4.9	4.9	5.0	5.0	4.9
22	4.9	4.9	4.9	5.0	5.0	4.9
MeO	–	–	4.00	3.98	3.97	3.36
R-gr	–	–	8.12	8.10	–	–
			7.62	7.59		
			7.45	7.51		

[a] Precision of ±0.03 ppm. Spectra at 25 °C, and alkaloid concentrations of 0.02 M. A, deoxycinchonidine in C_6D_6. B, deoxycinchonidine in $CDCl_3$. C, benzoylquinine in CD_3OD. D, benzoylquinine in $CDCl_3$. E, chloroquinine in $CDCl_3$. F, chloroquinine in C_6D_6.

Although temperature- and solvent-dependent NOESY and NOE-difference measurements did not reveal sufficient information to calculate exact ratios of distribution among possible conformations in solution, it is clear that in case of *deoxycinchonidine* both open conformation 3 as well as closed conformation 1 are present in C_6D_6 in about 60/40 ratio. As a specific example of the procedures that have been followed during the NMR study we describe in some detail how this conclusion was reached for the particular case of deoxycinchonidine. Thereafter only the main results for the other cinchona alkaloids will be given.

Assignment of ^{1}H NMR Spectral Data of Deoxycinchonidine. A 300-MHz ^{1}H NMR spectrum of deoxycinchonidine in C_6D_6 is shown in Figure 3. The chemical shift assignments are presented in Table II. See Figure 1 for the proton numbering. The aromatic H_1 and H_2 hydrogens are located as doublets at δ 6.93 and 8.81, re-

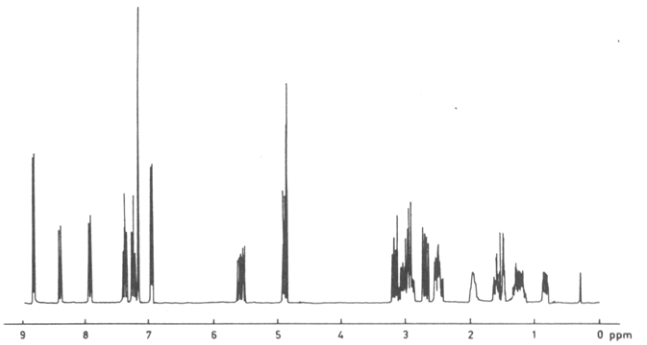

Figure 3. 300-MHz ^1H NMR spectrum of deoxycinchonidine in C_6D_6.

spectively, with an ortho coupling of 4.3 Hz. The H_3 proton appears as a doublet at δ 8.39 with an ortho coupling of 8.5 Hz to H_4, which appears as a multiplet at δ 7.37. As a result of a meta fine coupling of 0.9 Hz, the doublet of H_3 is further split by H_6, which appears as a multiplet at δ 7.24. H_5 at δ 7.93 appears as a doublet, owing to an ortho coupling of 8.4 Hz with H_6. In addition, a fine coupling of 0.9 Hz was observed, due to a meta coupling with H_4. The vinyl proton H_{20} appears as a multiplet at δ 5.58 and both terminal vinyl protons H_{21} and H_{22} as a multiplet at δ 4.90. The assignments of the quinuclidine protons were less straightforward. The benzylic C_9 carbon is substituted with two hydrogens. The hydrogen that replaces the hydroxy group in the case of cinchonidine is called H_{8b}, the other benzylic hydrogen H_{8a}. Both H_{8a} and H_{8b} appear as four lines at δ 3.15 and 2.69, respectively. The geminal H_{8a}–H_{8b} coupling is 7.8 Hz. In addition H_{8a} and H_{8b} have vicinal couplings with H_9 at δ 3.03 of 6.6 and 7.4 Hz, respectively. The COSY spectrum reveals that H_9 is coupled with the vicinal protons H_{10} and H_{11} at δ 1.60 and 0.83. Because of the stronger NOE between H_9 and H_{10} than between H_9 and H_{11}, the cis hydrogen H_{10} could be assigned to δ 1.60, thereby locating the trans hydrogen H_{11} at δ 0.83. Irradiation of H_9 yielded a NOE at δ 2.51, which was assigned to the nearest methylene proton H_{18}. This proton yields a strong NOE at δ 2.95 and a weaker enhancement at δ 1.94. These two signals were assigned to H_{19} and H_{17}, respectively, the former giving the strongest NOE due to its geminal relationship with H_{18}. The NOE between H_{18} and H_{20} supports the H_{18} assignment. The strong NOE between H_{19} and H_{17}, due to their cis relationship, is also in accordance with the assignments thus far. H_{17} shows two upfield NOE's at δ 1.48 and 1.18, which were assigned to H_{12} and H_{13}, respectively. Due to the geminal H_{13}–H_{14} relationship the strong NOE at δ 1.29 has been assigned to H_{14}. Because of both cis relationships H_{13}–H_{15} and H_{14}–H_{16}, revealed by strong NOE's, H_{15} could be assigned to δ 2.46 and H_{16} to δ 2.89. The *W* couplings between H_9 and H_{15} and between H_{10} and H_{13}, apparent in the COSY spectrum, support the assignments.

The ^1H NMR spectrum of deoxycinchonidine in $CDCl_3$ has also been recorded. The chemical shifts were obtained in a similar manner and are summarized in Table II.

Conformational Assignment of Deoxycinchonidine. The gross conformation of the cinchona alkaloids is determined by the torsions of the C_8–C_9 and C_9–C_4' bonds. The strategy has been to use interring NOE's in order to establish the overall conformation. These interring NOE's between quinoline hydrogens and quinuclidine hydrogens are important because they reveal the spatial relationship between both rings and thus the overall conformation of the alkaloid. NOESY and NOE-difference spectra have been recorded in order to obtain these interring NOE's. The results of a molecular mechanics study[7] were very helpful for the interpretation of the spectra. A schematic drawing of the closed conformation 2 and open conformation 3 for quinine derivatives is given in Figure 4. In this figure the arrows mark the hydrogens between which interring NOE's are expected for the conformation in question.

With the complete assignment of all hydrogens of deoxycinchonidine in C_6D_6 and $CDCl_3$ in hand, we next investigated the conformational behavior of this alkaloid in both solvents. The presence of closed conformation 2 in C_6D_6 could be excluded, because no NOE is observed between H_{16} and H_5. The absence of an Overhauser enhancement is a nonobservation and not a strong structural argument. However, we know from the conformational analysis of ester derivatives[7] that in the case of closed conformation 2 a strong NOE between H_{16} and H_5 (see Figure 4) is a characteristic of this conformation. Based on the same argument also open conformation 4 could be excluded, because no NOE was found between H_5 and H_{11}. From the epicinchona alkaloids (which adopt this open conformation 4) we know that a strong NOE is present[7] between H_5 and H_{11} in case of the open conformation 4. On the other hand, the NOE's observed between H_{11} and H_1, H_9 and H_5, H_{16} and H_{8a}, H_{8a} and H_5 and H_{8b} and H_{11} indicate that open conformation 3 must be present. But NOE's between H_{8b} and H_5, H_9 and H_5, H_{8a} and H_{11}, and H_{16} and H_1 were also found. These are all in accordance with closed conformation 1. Thus both open conformation

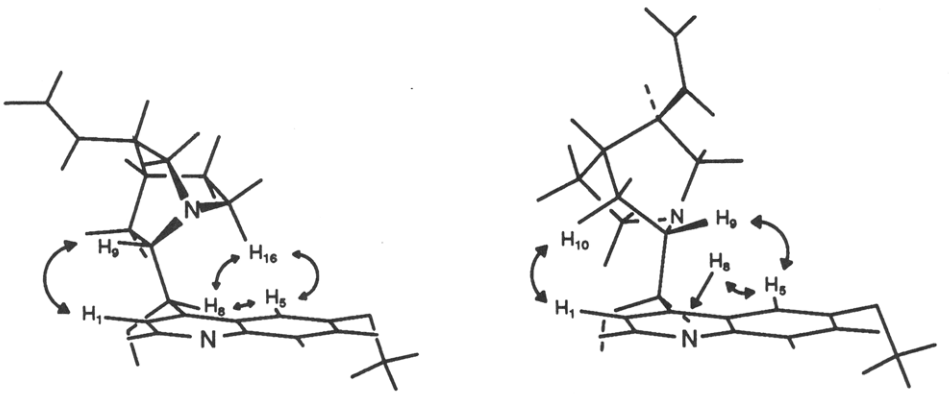

Figure 4. The closed conformation 2 and open conformation 3 of quinine and quinine derivatives. The arrows mark the hydrogens between which interring NOE's are expected to be found.

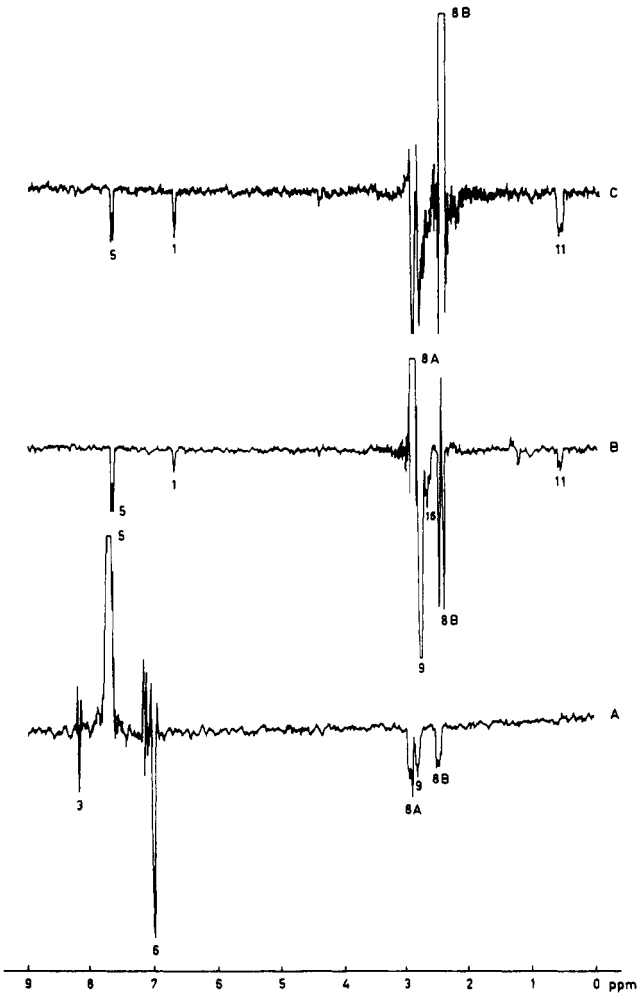

Figure 5. Traces of the 300-MHz NOESY spectrum of deoxycinchonidine in C_6D_6. A, H_5-trace; B, H_{8a}-trace; C, H_{8b}-trace.

3 as well as closed conformation 1 are present at the same time in a solution of C_6D_6. On the NMR time scale these two conformers exchange rapidly, because only an averaged ^1H NMR spectrum is recorded at 25 °C (Figure 3). In Figure 5A the trace of the NOESY, which shows the NOE interactions with H_5, is depicted. The enhancement marked 8A is due to NOE between H_5 and H_{8a} in open conformation 3, and the one marked 8B is due to a NOE between H_5 and H_{8b} in the closed conformation 1. We know from the molecular mechanics analysis that the interatomic H_5–H_{8a} distance in the open conformation 3 and the H_5–H_{8b} distance in the closed conformation 1 are approximately the same (about 2.1 Å). Thus integration of both enhancements 8A and 8B gives an approximate estimation of the ratio of distribution between both conformers. In Figure 5, parts B and C, the traces of hydrogens H_{8a} and H_{8b} are shown. In case of the H_{8a} trace, a relatively large NOE with H_5 and a smaller one with H_1 are observed. In case of the H_{8b} trace, both H_{8b}–H_5 and H_{8b}–H_1 enhancements are of the same order of magnitude. From the integration of these NOE traces we conclude that a ratio of approximately 60/40 exists between open conformation 3 and closed conformation 1.

^1H NMR and NOESY spectra of deoxycinchonidine have also been recorded in $CDCl_3$. Because of complete overlap in the ^1H NMR of protons H_9 and H_{16} (Table II) the presence of conformations 2 and 4 could not be excluded, but because of NOE's between H_1 and H_{8a}, H_1 and H_{8b}, H_5 and H_{8a}, H_5 and H_{8b}, and H_1 and H_{11}, it is clear that also in $CDCl_3$ a mixture of conformers is present, which must include conformers 1 and 3. Low-temperature experiments at −20 °C and −60 °C in $CDCl_3$ did not alter the ^1H NMR spectra; no line broadening has been observed, and averaged spectra were still recorded at −60 °C. Thus even at these low temperatures it was not possible to freeze out the different conformers. This is indicative of a fast exchange between the different conformations on the NMR time scale and thus of a low-energy barrier.

Conformational Assignments of the Other Cinchona Alkaloids. Based on arguments as outlined above we will now briefly summarize the results, which have been obtained for the other cinchona alkaloids.

The *hydroxy cinchona alkaloids* (quinine, quinidine, cinchonine, cinchonidine) all adopt predominantly the open conformation 3, but some conformational freedom of the quinuclidine ring is revealed by small NOE's between H_9 and H_1 and H_8 and H_{11} for the case of quinine and cinchonidine, and between H_9 and H_1 and H_8 and H_{10} for quinidine ahd cinchonine. These NOE's are indicative for closed conformation 2. However, a NOE between H_{16} and H_5 (quinine, cinchonidine) or H_{18} and H_5 (quinidine, cinchonine) was never observed. It is therefore concluded that the hydroxy cinchona alkaloids must exist at least for more than 90% in open conformation 3, wherein some conformational freedom of the quinuclidine ring exists.

Methoxy derivatives predominantly adopt the open conformation 3 and to a lesser amount the closed conformation 2 in $CDCl_3$. However, in CD_2Cl_2 the closed conformation 2 is found in excess. Thus now the distinct preference for the open conformation 3, seen for the hydroxy alkaloids, has vanished. In solvents like $CDCl_3$ and CD_3OD the open conformer 3 is still predominantly found, but in the noncoordinative solvent CD_2Cl_2 it is the closed conformer 2 that predominates. These observations are also reflected in the ^1H NMR spectra of the methoxy derivatives. In the ^1H NMR of methoxydihydroquinidine in $CDCl_3$ H_{11} appears at δ 1.13, whereas in CD_2Cl_2 H_{11} is found at δ 1.50, and this change in chemical shift (caused by the absence of shielding by the quinoline ring in the closed conformation 2) was accompanied by a substantial increase in the $^3J(H_8H_9)$ from 3.9 to 6.6 Hz.

The conformational assignments for the two *ester* derivatives (*p*-chlorobenzoyl)dihydroquinidine and (*p*-chlorobenzoyl)dihydroquinine in $CDCl_3$, CD_3COCD_3, CD_2Cl_2, CD_3CN, and $C_6D_5CD_3$ were described earlier.[7] It was concluded that in all these solvents the ester derivatives are in the closed conformation 2. Although recent examinations of NOESY spectra of benzoylquinine in $CDCl_3$ clearly demonstrated the existence of closed conformation 2, from the additional appearance of NOE's between H_1 and H_{11}, H_8 and H_9, and between H_{16} with the ortho protons of the benzoyl moiety, it is apparent that also the open conformation 3 occurs to the extent of 30–50%. Reinvestigation of other ester derivatives revealed that also for these compounds small amounts (about 30%) of open conformation 3 exist. From the NOESY spectra of benzoylquinine in CD_3OD it follows that the equilibrium between both conformers 2 and 3 is shifted in favor of the open conformation 3. This is also reflected by a decrease of the $^3J(H_8H_9)$ coupling constant from 6.4 to 5.1 Hz in $CDCl_3$ and CD_3OD, respectively.

Chloroquinine derivatives adopt for at least 90% the closed conformation 2 in C_6D_6, $CDCl_3$, and CD_3OD. The presence of small amounts of the open conformation 3 are revealed, however, by a very weak NOE betwen H_1 and H_{11}. This weak enhancement could only be detected by selective irradiation of hydrogen H_1 (thus not in the NOESY spectrum). From earlier obtained results[7] we

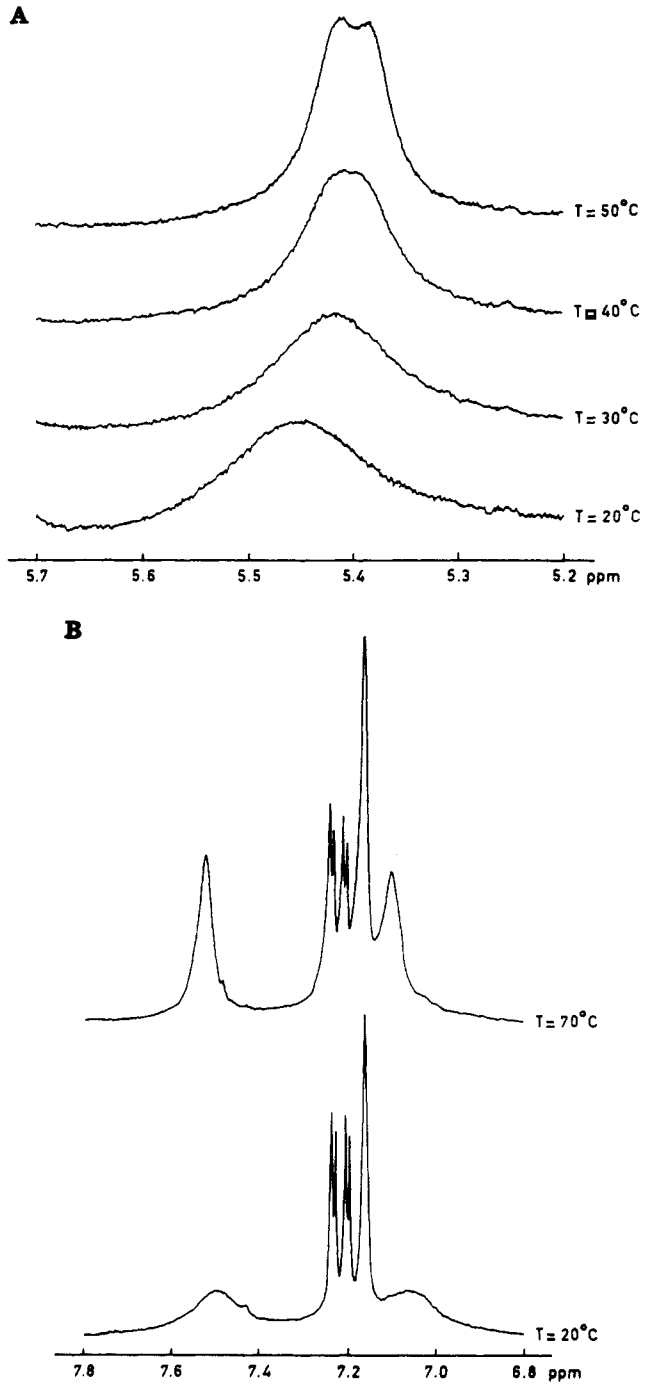

Figure 6. ^1H NMR spectra of chloroquinine at different temperatures. A, absorption of H_9 at 20, 30, 40, and 50 °C in $CDCl_3$. B, H_1, and H_5 absorptions at 20 and 70 °C in C_6D_6.

know that methoxy and ester cinchona derivatives adopt the open conformation 3 upon protonation of the quinuclidine nitrogen. We examined whether this conformational transition from the closed conformation 2 to the open conformation 3, induced by protonation, also occurs in case of chloroquinine. The conformational transition could not be induced, as with methoxy and ester derivatives, by the solvent CD_3OD. NOESY spectra of chloroquinine with 1 equiv DCl in CD_3OD revealed that, although the quinuclidine nitrogen is protonated, again no conformational transition is induced. That the quinuclidine nitrogen is at least partly protonated, follows from the upfield shifts of the α-protons of the quinuclidine nitrogen (H_9 shifts 0.98 ppm upfield, H_{16} 0.88 ppm, and H_{19} 0.52 ppm upfield). But there is still another interesting

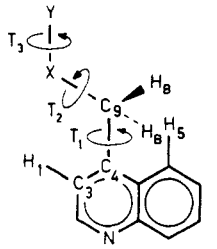

Compound	X	Y
A	H	–
B	O	H
C	O	Me
D	O	C(=O)–Me
E	Cl	–

Figure 7. Structures of the model compounds. $T_1 = C_3C_4C_9X$, $T_2 = C_4C_9XY$, and in case of compound D: $T_3 = C_9OC(O)C(H_3)$.

feature: all protons in the ^1H NMR spectra of the cinchona alkaloids discussed so far appear as sharp absorptions. But in case of chloroquinine in C_6D_6 and in $CDCl_3$ only the hydrogens H_1, H_5, H_8, and H_9 no longer appear as sharp absorptions, but as broad lines. The line broadening is caused by coalescence, which is shown in Figure 6. In Figure 6A the absorption of the benzylic hydrogen H_9 is shown at 20, 30, 40, and 50 °C, respectively, in $CDCl_3$. In Figure 6B the absorptions of both quinoline protons H_1 and H_5 are depicted at 20 and 70 °C in C_6D_6. These observations indicate that, only for the case of a chloro substituent at C_9, the energy barrier between closed conformation 2 and open conformation 3 is increased to such a height that at room temperature averaged spectra are no longer recorded. Attempts to observe this phenomenon for the other cinchona alkaloids by recording spectra at low temperatures (down to −60 °) did not lead to any observable line broadening.

MO Analysis

The NMR study of the cinchona alkaloids revealed that both the substituent at C_9, as well as the configuration at this position, play crucial roles in determining the conformational behavior.[10] Model compounds have been used for a calculation approach to elucidate the role of the benzylic position C_9. The structures of the model compounds, which are characterized by five different substituents R at C_9 are given in Figure 7. Each model compound resembles one of the cinchona alkaloid derivatives that we have studied. The geometries of the five model compounds were constructed in CHEMX[11] and optimized with MMP2.[12] Thereafter the geometries were refined with the VAMP[13] molecular orbital package using the AM1 Hamiltonian[14] by optimization over all internal coordinates. All subsequent calculations were also performed with VAMP (using the AM1 Hamiltonian).

(10) Epi-hydroxycinchona alkaloids, which have the opposite configuration at C_9 with respect to their parent compounds, adopt the open conformation 4, see ref 7.
(11) CHEMX, developed and distributed by Chemical Design Ltd., Oxford, England.
(12) QCPE Program 395/400. Allinger Force Field Molecular Mechanics Calculations, Allinger, N. L., Ed., Department of Chemistry, University of Georgia, Athens, GA 30602.
(13) VAMP: Erlangen Vectorized Molecular Orbital Package, version 4.10 (based on AMPAC 1.0 and MOPAC 4.0)
(14) AM1: Dewar, M. J. S. *J. Am. Chem. Soc.* **1985**, 3902.

Table III. Results of AM1 Optimizations for All Model Compounds

	OH-0-180	OH-120-180	OH-0-60	OH-120-60	OMe-0-180	OMe-120-180	OMe-0-80	OAc-0-180-0	OAc-120-180-0	OAc-0-180-180	OAc-0-60-180	OAc-120-180-180	Cl-0	Cl-120
energy (kcal/mol)	2.6	3.9	0.3	0.9	6.6	7.8	5.7	-30.8	-29.3	-36.4	-36.2	-35.4	39.5	39.0
T_1	0.1	121.5	7.0	125.8	2.4	120.3	6.7	0.0	119.6	0.1	2.0	116.4	1.8	102.6
T_2	180.0	170.5	-62.2	-53.1	174.0	180.1	81.9	179.9	182.8	180.5	104.7	198.1	1.754	1.758
T_3	-	-	-	-	-	-	-	-0.1	1.7	179.8	181.2	179.0	-	-
C9O	1.421	1.421	1.413	1.415	1.429	1.429	1.432	1.432	1.432	1.439	1.431	1.439	-	-
C9H	1.126	1.126	1.126	1.126	1.125	1.125	1.125	1.125	1.125	1.124	1.125	1.124	1.120	1.118
C4'C9	1.494	1.497	1.495	1.497	1.493	1.495	1.495	1.493	1.495	1.491	1.494	1.494	1.486	1.484
C4'C9O	109.3	109.2	113.6	113.8	109.1	108.8	113.5	108.5	108.6	108.7	111.5	107.9	115.3	112.0
C4'C9H	109.7	109.9	109.9	110.1	110.1	110.4	109.8	110.1	110.2	111.0	110.2	111.2	110.0	111.2
C3'C4'C9	121.9	119.8	121.6	120.0	122.1	119.8	121.8	122.2	119.6	122.7	122.3	119.7	123.6	119.8

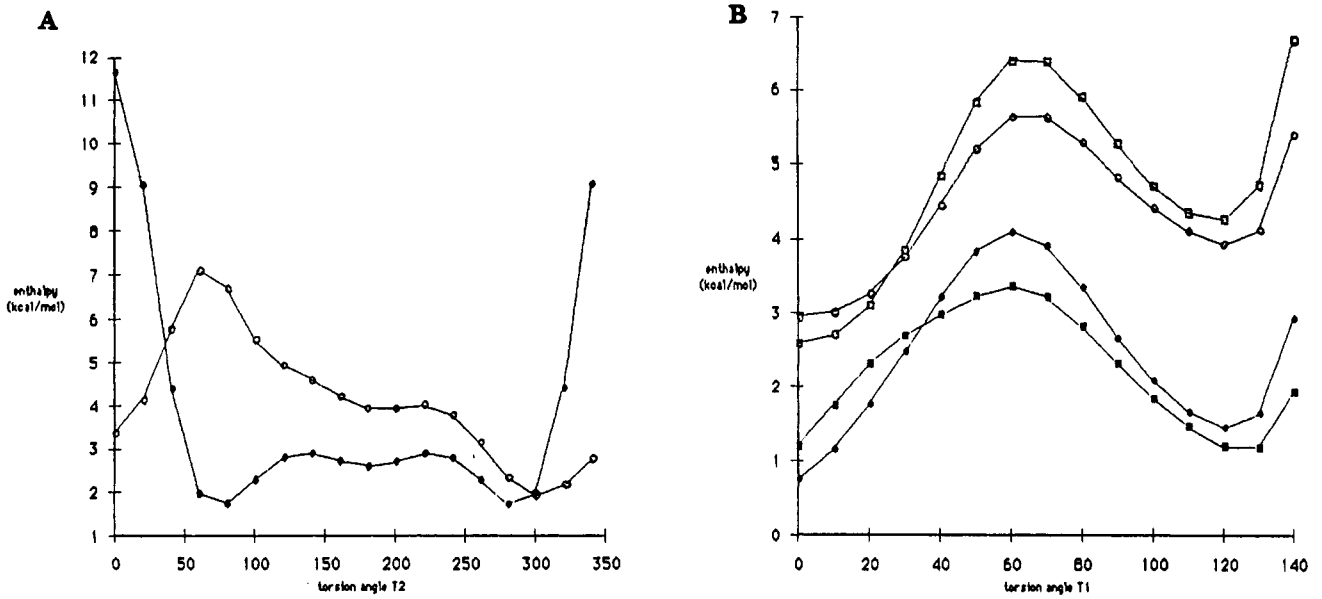

Figure 8. (A) Enthalpy dependence of T_2 for model compound B. (●), the enthalpy as function of T_2 for OH-0-180; (○), for OH-120-180. (B) Enthalpy dependence of T_1 for model compound B. (●), the enthalpy as a function of T_1 for OH-0-180; (○), the OH-0-300; (■), for OH-120-180; and (□), for OH-120-300.

Compound A. The enthalpy dependence on the torsion angle T_1 has been computed by varying T_1 in steps of 10° (see Figure 7 for the definition of T_1). In the optimized starting geometry $T_1 = 0°$. At each point the enthalpy has been calculated. The resulting plot of the enthalpy against T_1 reveals three minimum energy conformations at $T_1 = 0$, $T_1 = 120$, and $T_1 = 240°$, all three of which are identical because of symmetry. The minima place one of the benzylic protons in the same plane as the quinoline proton H_1. The energy barriers of 2.3 kcal/mol at $T_1 = 60$, 180, and 300° are caused by steric repulsion between one of the benzylic protons and the quinoline proton H_5.

Compound B. Two conformations have been optimized, one called OH-0-180, starting with $T_1 = 0°$ and $T_2 = 180°$, and one called OH-120-180, starting with $T_1 = 120°$ and $T_2 = 180°$. Some results of these optimizations are summarized in Table III. The calculations predict conformation OH-0-180, with the hydroxy oxygen oriented in the plane of the quinoline ring and directed toward H_1 (Figure 7) to be 1.3 kcal/mol more stable than conformer OH-120-180, in which one of the benzylic protons occupies this position.

Next, the preferred orientation of the hydroxyl proton has been investigated. For both OH-0-180 and OH-120-180 T_2 was varied in steps of 20° and the AM1 energy has been calculated at each point. The results of these calculations are summarized in plots of enthalpy against T_2, depicted in Figure 8A. From these plots it follows that the orientation of the hydroxyl proton is able to affect the enthalpy considerably. For OH-0-180 two absolute minimum energy conformations exist at approximately $T_2 = 60°$ and $T_2 = 300°$. One relative minimum is found at approximately $T_2 = 180°$. This staggered conformation has both oxygen lone pairs oriented between a C–C and a C–H bond, whereas in the two absolute minima the two oxygen lone pairs are situated between two C–H bonds, which leads to less electronic repulsion. In the case of OH-120-180 the staggered conformer with $T_2 = 60°$ is an energy maximum, because of steric repulsion between the hydroxyl proton and H_5 of the quinoline ring.

The geometries of both OH-0-180 and OH-120-180 have been optimized again, but now starting with $T_2 = 300°$. The resulting conformations are called OH-0-300 and OH-120-300, respectively. In table III the most important results of these optimizations are summarized. It follows that the energy difference between conformers with $T_1 = 0°$ and $T_1 = 120°$ decreases from 1.3 to 0.5 kcal/mol upon changing T_2 from 180° to 300°.

Next, all four optimized geometries have been used as starting conformers to study the energy dependance on T_1. Of special interest is plot B of Figure 8B. This plot shows the enthalpy dependence on T_1 for OH-0-300. Conformer OH-0-300 resembles the open conformation 3 of quinidine. In the closed conformation 2 of quinidine T_1 changes from about 0 to 60°. Thus the height of the energy barrier of plot B of Figure 8B at $T_1 = 60°$ relative to $T_1 = 0°$ is important, because it reflects the amount of destabilization in going from the open conformation 3 to the closed conformation 2. These calculations predict an energy difference of 3.5 kcal/mol.

Compound C. Two conformations have been optimized, one called OMe-0-180, starting with $T_1 = 0°$ and $T_2 = 180°$,

Table IV. Results of AM1 Optimizations on the Closed Conformation 2 and Open Conformation 3 of Some Quinidine Derivatives

	C4–C9 (Å)	C9–R (Å)	C9–H (Å)	C3C4C9	C4C9R	C4C9C8	enthalpy (kcal/mol)
OH closed 2	1.504	1.428	1.125	118.61	110.54	111.91	-9.4
OH open 3	1.506	1.423	1.130	120.34	111.07	110.34	-11.4
OMe closed 2	1.504	1.436	1.124	118.81	110.40	111.48	-3.8
OMe open 3*	1.506	1.431	1.129	120.72	110.86	110.09	-4.7
OAc closed 2	1.502	1.447	1.124	118.93	106.37	112.31	-45.8
OAc open 3	1.504	1.439	1.130	121.06	109.42	110.01	-46.1
Cl closed 2*	1.492	1.779	1.120	119.65	109.08	112.80	27.5
Cl open 3	1.498	1.775	1.124	121.23	109.94	110.21	29.3

and one called OMe-120-180, starting with $T_1 = 120°$ and $T_2 = 180°$. Some results of these optimizations are summarized in Table III. Conformer OMe-0-180 with the oxygen oriented in the plane of the quinoline ring and directed toward H_1 is predicted to be 1.2 kcal/mol more stable than conformer OMe-120-180.

The energy dependence for OMe-0-180 as a function of T_2 has been calculated by stepwise variation of T_2 in steps of 10°. The results of these calculations suggest that one absolute minimum exists at approximately $T_2 = 180°$. The other two staggered conformations at approximately $T_2 = 80°$ and $T_2 = 270°$ are relative minima.

Conformation OMe-0-180 was optimized again, this time starting with $T_2 = 80°$. The optimized geometry is called OMe-0-80, and some results are summarized in Table III. Thus after optimization over all internal coordinates OMe-0-80 turns out to be 0.9 kcal/mol more stable than OMe-0-180. Because conformer OMe-0-80 resembles the open conformation 3 of the methoxy derivative of quinidine the enthalpy dependence on T_1 was further investigated. Both in OMe-0-80 and OMe-0-180 T_1 has been varied in steps of 10° and the AM1 energy has been computed at each point. The results of these calculations are summarized in the plots of Figure 9. In case of OMe-0-80 the energy barrier in going from $T_1 = 10°$ to $T_1 = 60°$ is estimated to be 3.1 kcal/mol.

Model Compound D. The three important dihedrals of D are defined in Figure 7. An analysis similar to that described for the other model compounds has been followed. First, five conformations have been optimized; OAc-0-180-0 ($T_1 = 0°$, $T_2 = 180°$, $T_3 = 0°$); OAc-120-180-0 ($T_1 = 120°$, $T_2 = 180°$, $T_3 = 0°$); OAc-0-180-180 ($T_1 = 0°$, $T_2 = 180°$, $T_3 = 180°$); OAc-120-180-180 ($T = 120°$, $T_2 = 180°$, $T_3 = 180°$); and OAc-0-60-180 ($T_1 = 0°$, $T_2 = 60°$, $T_3 = 180°$). The most important results of these optimizations are summarized in Table III.

An energy analysis of T_3 showed a 2-fold potential with minima at $T_3 = 0°$ and $T_3 = 180°$. From Table III it is clear that a distinct preference exists for $T_3 = 180°$ (ranging from 5.6 to 6.1 kcal/mol). Both optimized geometries OAc-0-60-180 and OAc-0-180-180 have been used to study the energy dependence on T_1. Different conformations were generated by varying T_1 in steps of 10°. From the resulting plots of Figure 10 it follows that the energy barrier of conformer OAC-0-60-180 (which resembles acetylquinidine) in going from $T_1 = 0°$ to $T_1 = 60°$ is 2.6 kcal/mol.

Model Compound E. Two conformations have been optimized, one starting with $T_1 = 0°$ called Cl-0 and one starting with $T_1 = 120°$ called Cl-120. Table III summarizes the most important results of these optimizations. This time not the conformer with $T_1 = 0°$ is found to be the absolute minimum, but instead Cl-120 with $T_1 = 120°$ is calculated to be 0.5 kcal/mol more stable. The calculated energy dependence on T_1, using the optimized conformation Cl-0 as starting geometry is given in Figure 11. The energy barrier in going from $T_1 = 0°$ to $T_1 = 60°$ is estimated to be 3.0 kcal/mol.

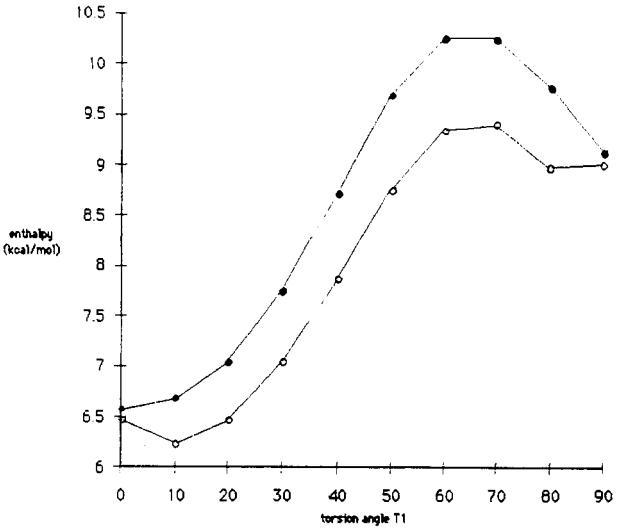

Figure 9. Enthalpy dependence of T_1 for model compound C. (○), the enthalpy as function of T_1 for OMe-0-80; (●), for OMe-0-180.

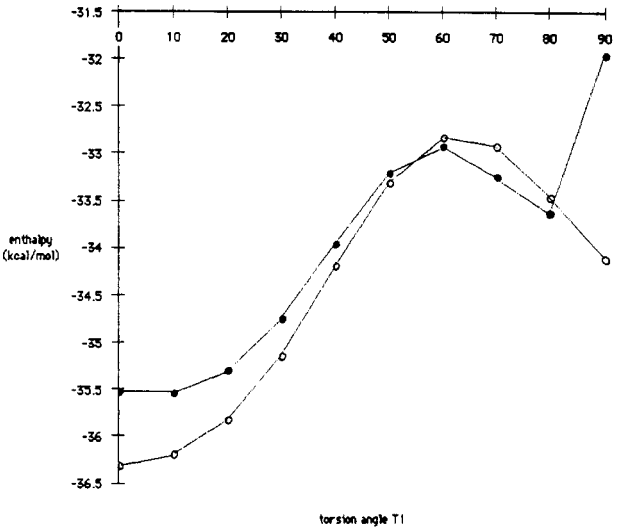

Figure 10. Enthalpy dependence of T_1 for model compound D. (●), the enthalpy as a function of T_1 for OAc-0-60-180; (○), for OAc-0-0-180.

Cinchona Alkaloids. Some optimizations have been performed on the complete structure of cinchona alkaloids. Starting conformations obtained from the molecular mechanics calculations have been used for the optimizations over all internal coordinates. The cinchona alkaloids that have been considered as summarized in Table IV, together with the most important results.

Effect of C_9–H Bond Length and $C_4'C_9H$ Bond Angle. The results of the calculations described above show that the C_9–H bond length is affected by the nature of the benzylic substituent R. In going from R = OH, OMe, OAc, Cl, H the C_9–H bond length decreases from 1.126 to 1.118

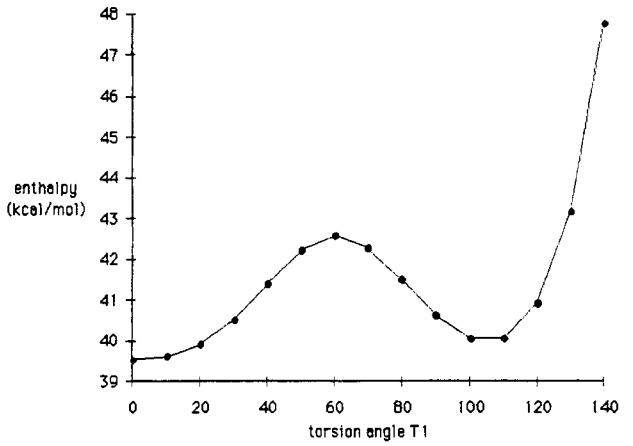

Figure 11. Enthalpy as a function of T_1 for model compound E.

Å. In an attempt to investigate the influence of this bond length on the height of the energy barrier, caused by benzylic H–H_5 repulsion, the C_9–H bond length was systematically varied from 1.110 to 1.130 Å in steps of 0.002 Å. In these calculations the geometry of OH-0-180 has been used as basic geometry. At each bond length the height of the energy barrier has been computed by stepwise variation of T_1. No significant effect on the benzylic H–H_5 repulsion could be detected.

The $C_4'C_9H$ bond angle is also affected by the nature of the benzylic substituent. In order to investigate the influence of this bond angle on the benzylic H–H_5 repulsion, the height of the energy barrier has been calculated for $C_4'C_9H$ bond angles of 109 and 112°, together with C_9H bond lengths of 1.110, 1.120, and 1.130 Å, respectively. Again the geometry of OH-0-180 has been used as basic geometry for these calculations. In Figure 12A only the results of the calculations with a C_9H bond length of 1.120 Å are given, results for the other two bond length were very similar. Thus decreasing the bond angle from 112 to 109° causes an increase of the benzylic H–H_5 repulsion of about 0.4 kcal/mol.

Effect of C_9O Bond Length and $C_4'C_9O$ Bond Angle. In going from R = OH, R = OMe, R = OAc the C_9O bond length tends to increase from about 1.140 to 1.145 Å, whereas the $C_4'C_9O$ bond angle tends to decrease (see Table 3). To study the effect of this bond length and angle on the interaction between oxygen and the quinoline proton H_1 four energy plots have been calculated. The geometry of OH-0-180 has been used as starting conformation in all calculations. The results of the calculations are summarized in Figure 12B. Plot A gives the energy curve for $C_4'C_9O$ = 108° and C_9O = 1.140 Å; plot B for $C_4'C_9O$ = 108° and C_9O = 1.145 Å; plot C for $C_4'C_9O$ = 112° and C_9O = 1.140 Å; plot D for $C_4'C_9O$ = 112° and C_9H = 1.145 Å. From these plots it follows that the enthalpy decreases only about 0.03 kcal/mol when the C_9O bond length increases from 1.140 to 1.145 Å, whereas increasing the $C_4'C_9O$ bond angle from 108 to 112° causes a stabilization of the minimum energy conformation of T_1 = 0° of about 0.3 kcal/mol.

Effect of the $C_3'C_4'C_9$ Bond Angle. The VAMP calculations on the model compounds as well as on the complete cinchona alkaloids have shown that the $C_3'C_4'C_9$ bond angle is strongly affected by the benzylic substituent R (variation from 118.8 to 123.5°). Probably this is to reduce steric repulsion between the quinoline proton H_1 and the benzylic substituent R. The $C_3'C_4'C_9$ bond angle increases when the C_9O bond length tends to increase or when the $C_4'C_9O$ bond angle tends to decrease.

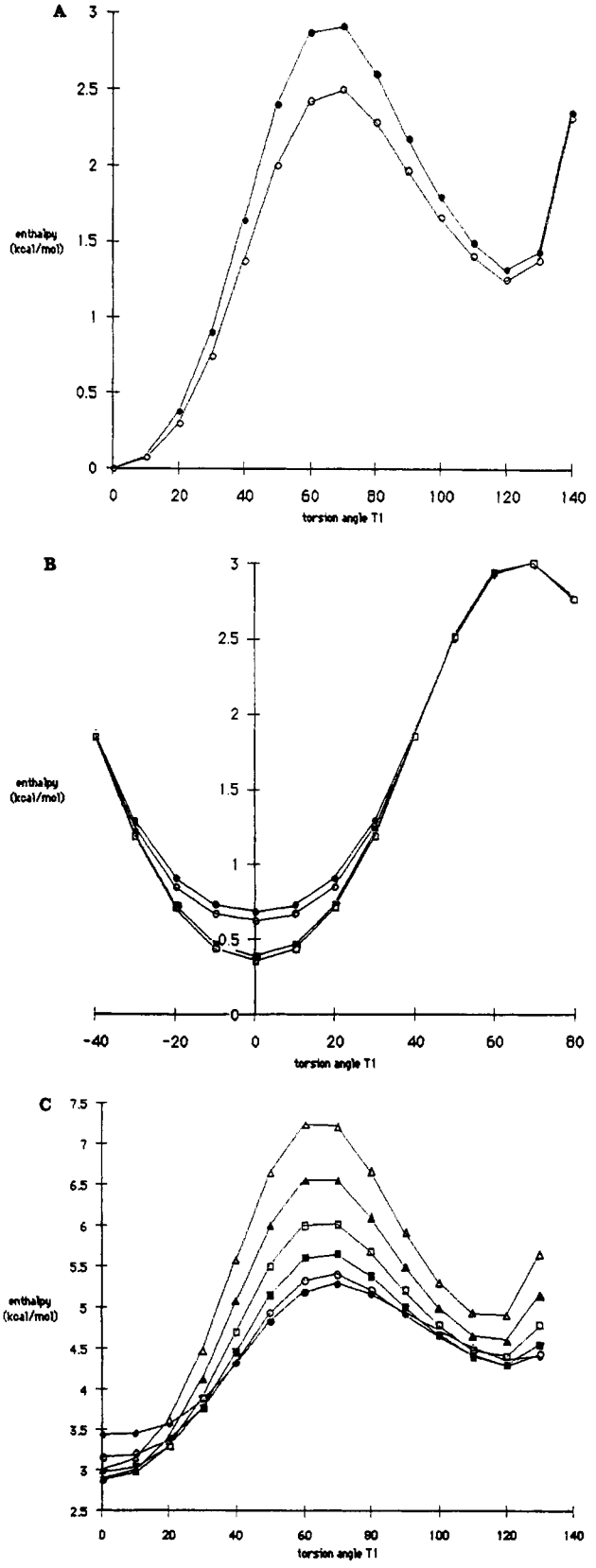

Figure 12. (A) Enthalpy as a function of T_1. (●), for the OH-0-180 basic geometry with $C_4'C_9H_8$ = 109° and C_9H = 1.120 Å the enthalpy is plotted against T_1; (○), for $C_4'C_9H_8$ = 112° and C_9H = 1.120 Å. (B) Enthalpy as a function of T_1. (●), for the OH-0-180 basic geometry with $C_4'C_9O$ = 108° and C_9O = 1140 Å; (○), with $C_4'C_9O$ = 108° and C_9O = 1.145 Å; (■), with $C_4'C_9O$ = 112° and C_9O = 1.140 Å; (□), with $C_4'C_9O$ = 112° and C_9O = 1.145 Å. (C) Enthalpy as a function of T_1. (●), for the OH-0-180 basic geometry with $C_3'C_4'C_9$ = 118.5°; (○), with $C_3'C_4'C_9$ = 119.5°; (■), with $C_3'C_4'C_9$ = 120.5° (□), with $C_3'C_4'C_9$ = 121.5°; (▲), with $C_3'C_4'C_9$ = 122.5°; and (△), with $C_3'C_4'C_9$ = 123.5°.

Using the OH-0-189 basic geometry, T_1 has been varied from 0 to 130° in steps of 10°. This has been done for six different $C_3'C_4'C_9$ bond angles, ranging from 118.5 to 123.5°. The resulting six plots of enthalpy against T_1 are shown in Figure 12C. It follows that there exist two different effects on the enthalpy. First, decrease of the $C_3'C_4'C_9$ bond angle causes destabilization of the absolute minimum at $T_1 = 0°$ (increased steric interactions between O and H_1). This is a relatively small enthalpy effect (0.7 kcal/mol). Second, decrease of the $C_3'C_4'C_9$ bond angle causes a relatively large enthalpy effect on the benzylic $H-H_5$ repulsion, which decreases about 2 kcal/mol.

Discussion

If we examine the data for the T_1 dependence on the enthalpy of the model compounds that have been studied, it is easily concluded that all plots of enthalpy against T_1 are very similar. Three minima are located at approximately $T_1 = 0°$, $T_1 = 120°$, and $T_1 = 240°$. In all cases, except for the chloro model compound, the absolute minimum is found at about $T_1 = 0°$, whereas at about $T_1 = 120°$ and $T_1 = 240°$ relative minima are found. In all cases these three minima are separated by one large and two relatively small energy barriers. The two small energy barriers at approximately $T_1 = 60$ and $T_1 = 300°$ are caused by repulsion between the benzylic proton and H_5. The huge energy barrier is caused by repulsion between the benzylic R substituent and H_5.

In the open conformation 3 of the cinchona alkaloids the benzylic substituent is situated in the same plane as the quinoline ring and directed toward H_1 (thus resembling the absolute minima of the model compounds). In the closed conformation 2 of the cinchona alkaloids the situation with respect to the benzylic substituents is different; one of the benzylic hydrogens is now oriented in the same plane as the quinoline ring and points toward H_5. The benzylic R substituent has turned about 60° out of the quinoline plane (thus resembling the relative maxima of the model compounds). In cases analogous to the open conformation 4 the benzylic subtituent R is also oriented in the quinoline plane, but now it points toward H_5 instead of toward H_1. From the calculational results we have seen that this is very unfavorable (high energy barrier) because of the relatively large repulsion between the benzylic R and H_5. The configuration at C_9 of the epicinchona alkaloids is opposite to that of the cinchona series, thus now closed conformation 2 and to a lesser extent open conformation 3 are unlikely for the same reason. Deoxycinchona alkaloids do not have a benzylic substituent and thus miss the discrimination caused by the configuration at C_9. In this light it is no surprise that deoxycinchona alkaloids are found both in conformation 1 and 3.

Some complete cinchona derivatives have also been optimized. The results of these calculations for quinidine predict the *open* conformation 3 to be 2.0 kcal/mol more stable than the closed conformation 2. For the methoxy derivative this energy difference decreases to 0.9 kcal/mol, and for acetylquinidine the energy difference decreases further to 0.3 kcal/mol. The chloro derivative in the *closed* conformation 2 is predicted by AM1 to be 1.8 kcal/mol more stable than in the open conformation 3. Ignoring the precise absolute magnitudes of the energy differences, we conclude that there exists excellent agreement between these calculational results and the experimental observations in solution and in the solid state. This suggests that the AM1 calculations are well suited to predict experimentally observed trends in energy differences between possible conformations of a given cinchona derivative and between the different derivatives of cinchona alkaloids.

However, the main object of our calculations is not to find good correlations between experimental observations and theoretical predictions, but to find explanations for the conformational behavior of the cinchona alkaloids. Let us return to the model compounds and concentrate on the benzylic $H-H_5$ and benzylic $R-H_1$ repulsions. The calculations on the model compounds suggest the existence of a delicate balance between benzylic $R-H_1$ and benzylic $H-H_5$ interactions. Increase of the C_9R bond length or decrease of the $C_4'C_9R$ bond angle causes a decrease of the benzylic $R-H_1$ interatomic distance and thus an increased steric repulsion. This can be released by increasing the $C_3'C_4'C_9$ bond angle, but at the same time this has considerable consequences for the benzylic $H-H_5$ repulsion (Figure 12C). In going from R = OH, OMe, OAc the electron-withdrawing capacity of the R group increases, as a result the C_9O bond length increases. In the same order the $C_4'C_9O$ bond angle decreases. This explains why the situation resembling the open conformation 3 (T_1 is approximately 0°) will be destabilized going from R = OH, OMe, OAc. In the same time, for closed conformation 2 (T_1 is approximately 60°), the benzylic $H-H_5$ repulsion can be relieved significantly by decreasing the $C_3'C_4'C_9$ bond angle and to a lesser amount by increasing the $C_4'C_9H$ bond angle. Both trends are indeed present in going from R = OH, OMe, OAc, Cl. Thus the geometry resembling the closed conformation 2 will be stabilized in the same order

Solute–alkaloid interactions are another aspect. These too are able to influence the conformational behavior. In this article several examples have been mentioned, e.g., methoxyquinidine, which adopts predominantly the open conformation 3 in $CDCl_3$ and closed conformation 2 in CD_2Cl_2; benzoylquinidine, which predominantly adopts the closed conformation 2 in all solvents except CD_3OD, in which it is found chiefly in the open conformation 3. But also complexation with osmium tetraoxide[7] or protonation of the alkaloid is able to induce conformational transitions from the closed conformation 2 to the open conformation 3, except for chloroquinine, where this conformational transition could be induced even upon protonation. These examples clearly indicate that solute–alkaloid interaction are able to dictate the conformation only in certain circumstances. From NMR and X-ray data we know that it is the quinuclidine nitrogen which is responsible for the interactions with solvents (e.g. methanol, acetic acid) or electrophiles (e.g. aromatic thiol, osmium tetraoxide). Quantitative information about the enthalpy gain caused by these interactions is not available, but preliminary calculations suggest the magnitude of these to be in the order of 1–3 kcal/mol (and of course for these data entropy effects are not taken into account). In the closed conformation 2 of the cinchona alkaloids it is practically impossible, because of geometrical reasons, for the quinuclidine nitrogen lone pair to participate in alkaloid-solute interactions, whereas in case of the open conformation 3 the nitrogen lone pair is freely accessible to ligand or solute (this facet is implicit in our conformational terminology of "closed" or "open").

With all this information in hand we think that the picture is complete enough to propose an integral rationalization for the conformational behaviour of the cinchona alkaloids. Because of reasons discussed above chloro cinchona alkaloids adopt closed conformation 2 almost exclusively. The energy difference between closed conformation 2 and open conformation 3 is too large to be compensated by enthaply gain as a result of interactions between open conformation 3 of the chloro derivative with

solute or ligand. In case of ester derivatives the energy difference between closed and open conformation is less and is probably of the same order of magnitude as the amount of stabilization caused by interactions with solutes, such as methanol or weak acids, or with strong electrophiles, such as osmium tetraoxide. In case of the methoxy derivatives the energy difference between closed conformation 2 and open conformation 3 has vanished. In noncoordinating solvents like CD_2Cl_2, the methoxy derivatives are still predominantly found in the closed conformation 2, but in the presence of any electrophile the equilibrium shift in favor of the open conformation 3. Quinine and quinidine (and other hydroxy derivatives) by themselves already possess a distinct preference for the open conformation 3 and thus do not depend on extra stabilization caused by interactions with solute.

Experimental Section

The NOESY and COSY spectra were measured as 0.05–0.1 M solutions in a 5-mm NMR tube. In the case of the NOESY spectra the oxygen was removed by freeze–pump–thaw cycles and the NMR tubes were sealed under reduced pressure. All spectra (^1H NMR, COSY, NOE-difference, and NOESY) were recorded using a Varian VXR-300 and VXR-500 spectrometer at 20 °C. For each NOESY spectrum between 512 and 1024 FID's of between 1024 and 2048 data points each were collected. The spectral width was chosen as narrow as possible (about 3000 Hz). Corrections with weighting functions (mostly shifted sine bells[15]) were used before Fourier transformations in the t_2 and t_1 dimensions. All NOESY spectra were recorded in phase sensitive mode.[16] Energy calculations were performed on a Convex c210 computer with VAMP version 4.10, a vectorized molecular orbital package based on AMPAC 1.0 and MOPAC 4.10. All optimizations were performed either over all internal coordinates or the Cartesian coordinate system was used, until the root-mean-square of the gradient of the energy was less than 0.1 kcal/Å. All alkaloid derivatives were synthesized by literature procedures.

Acknowledgment. We express thanks for the use of the services of the Dutch CAOS-CAMM center under Grants SON-11-20-700 and STW-NCH-440703. Modeling and computer facilities were provided by Royal Dutch Shell.

Registry No. A, 491-35-0; B, 6281-32-9; C, 64218-83-3; D, 35982-82-2; E, 5632-17-7; dihydroquinine, 522-66-7; dihydroquinidine, 1435-55-8; dihydrocinchonine, 485-65-4; dihydrocinchonidine, 485-64-3; dihydromethoxyquinidine, 122898-88-8; benzoylquinine, 69758-70-9; dihydro-*p*-chlorobenzoylquinine, 113216-88-9; dihydro-*p*-chlorobenzoylquinidine, 113162-02-0; dihydroacetylquinidine, 72989-10-7; dihydrochloroquinine, 50412-62-9; dihydrochloroquinidine, 50412-64-1; deoxycinchonidine, 5808-37-7; epidihydroquinine, 51743-68-1; epidihydroquinidine, 14645-32-0; chloroquinine, 14528-48-4.

(15) Levitt, M. H.; Radloff, C.; Ernst, R. R. *Chem. Phys. Lett.* **1985**, *114*, 435.
(16) States, D. J.; Haberkorn, R. A.; Ruben, D. J. *J. Magn. Reson.* **1982**, *48*, 286.

Reversible Oxidation of Phosphylthionates and Phosphylselenonates with Trifluoroacetic Anhydride[1a]

Karol S. Bruzik*[,1b] and Wojciech J. Stec

Center of Molecular and Macromolecular Studies, Polish Academy of Sciences, Sienkiewicza 112, 90-362 Lodz, Poland

Received March 29, 1990

Trifluoroacetic anhydride oxidizes a variety of phosphylthionates and -selenonates into corresponding oxo products at room temperature. In the case of phosphine sulfide **1**, the reaction proceeds with complete racemization, while phosphine selenide **2** is oxidized with a net inversion and a high degree of racemization. The extent of epimerization during the oxidation of diastereomeric phosphoroselenonates is much lower. The variable-temperature ^{31}P NMR spectra show the existence of two intermediates: a phosphonium salt **12** and the pentacoordinated compound **13**, both originating from the acylation of the product at phosphoryl oxygen. Two analogous intermediates containing sulfur or selenium, occurring earlier on the reaction pathway, are also postulated. The entire process is fully reversible as evidenced by the conversion of ethylmethylphenylphosphine oxide into the corresponding sulfide during the desulfurization of methyl-*n*-propylphenylphosphine sulfide. The equilibrium is gradually shifted into the oxidized product by the decomposition processes of trifluorothio- or trifluoroselenoacetic anhydride.

The oxidation of phosphylthioates and phosphylselenoates into their corresponding oxo compounds has been the subject of considerable interest in this and other laboratories. The oxidation reagents applied included potassium permanganate,[2] nitric acid,[3] dinitrogen tetroxide,[4] hydrogen peroxide,[5,6] organic peracids,[7] ozone,[8] dimethyl sulfoxide,[9] and selenoxide.[10] More recently, the

Scheme I

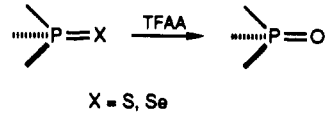

X = S, Se

stereospecific PS → PO conversion of phosphorothioyl analogues of nucleotides by using oxidative bromination[11,12] and [^{18}O]oxygen labeled epoxides[13] have been described. In the course of our earlier studies on the mechanism of the thiono–thiolo rearrangement of phosphylthionates in trifluoroacetic acid medium,[14,15] we have occassionally

(1) (a) Dedicated to Prof. Jan Michalski on his 70th birthday. (b) Current address: Chemistry Department, The Ohio State University, 140 W. 18th Ave., Columbus, OH 43210.
(2) Horner, L. *Pure Appl. Chem.* **1964**, *9*, 225.
(3) Stec, W. J.; Okruszek, A.; Michalski, J. *Angew. Chem.* **1971**, *83*, 491.
(4) Stec, W. J.; Okruszek, A.; Mikolajczyk, M. *Z. Naturforsch. B* **1971**, *26*, 856.
(5) Stec, W. J.; Okruszek, A.; Michalski, J. *J. Org. Chem.* **1976**, *41*, 233.
(6) De'ath, N. J.; Ellis, K.; Smith, D. J. H.; Trippett, S. *J. Chem. Soc., Chem. Commun.* **1971**, 714.
(7) Herriott, A. W. *J. Am. Chem. Soc.* **1971**, *93*, 3304.
(8) Skowronska, A.; Krawczyk. E. *Synthesis* **1983**, 509.
(9) Mikolajczyk, M.; Luczak, J. *Chem. Ind. (London)* **1974**, 701.
(10) Mikolajczyk, M.; Luczak, J. *J. Org. Chem.* **1978**, *43*, 2132.
(11) Conolly, B. A.; Eckstein, F.; Cullis, P. M. *J. Biol. Chem.* **1982**, *257*, 3382.
(12) Sammons, R. D.; Frey, P. A. *J. Biol. Chem.* **1982**, *257*, 1138.
(13) Guga, P.; Okruszek, A. *Tetrahedron Lett.* **1984**, *26*, 2897.

0022-3263/90/1955-6131$02.50/0